

Highly Active Titanocene Catalysts for Epoxide Hydrosilylation: Synthesis, Theory, Kinetics, EPR Spectroscopy

Dina Schwarz G. Henriques[†], Katharina Zimmer[†], Sven Klare[†], Andreas Meyer, Elena Rojo-Wiechel, Mirko Bauer, Rebecca Sure, Stefan Grimme, Olav Schiemann,* Robert A. Flowers II,* and Andreas Gansäuer*

Abstract: A catalytic system for titanocene-catalyzed epoxide hydrosilylation is described. It features a straightforward preparation of titanocene hydrides that leads to a reaction with low catalyst loading, high yields, and high selectivity of radical reduction. The mechanism was studied by a suite of methods, including kinetic studies, EPR spectroscopy, and computational methods. An unusual resting state leads to the observation of an inverse rate order with respect to the epoxide.

Epoxide hydrosilylations are virtually unexplored reactions that offer a simple access to alcohols.^[1] Epoxidation and titanocene-catalyzed^[2] epoxide hydrosilylation (Scheme 1) provide a two-step approach to the formal anti-Markovnikov addition of H₂O to olefins that circumvents hydroboration. However, it also highlights the difficulties associated with the reactive and relatively unstable titanocene(III) hydrides ([Cp₂TiH] hereafter). Their generation is capricious and requires either harsh conditions^[3] or the syntheses of sensitive complexes.^[4] Herein, we report a reliable and easy procedure for catalyst generation from titanocene dichlorides, mechanistic key features of the reaction, and EPR data for the species involved.

Our starting point was the *in situ* generation of [Cp₂TiH]. [Cp₂TiR] complexes are attractive in this context because of the weak Ti–C bond.^[5] We studied σ-bond metathesis of these complexes with PhSiH₃ and (EtO)₃SiH computationally (Figure 1).^[6]

[*] D. S. G. Henriques,^[†] K. Zimmer,^[†] S. Klare,^[†] E. Rojo-Wiechel, Prof. Dr. A. Gansäuer
Kekulé-Institut für Organische Chemie und Biochemie
Universität Bonn
Gerhard-Domagk-Straße 1, 53121 Bonn (Deutschland)
E-mail: andreas.gansaeuer@uni-bonn.de

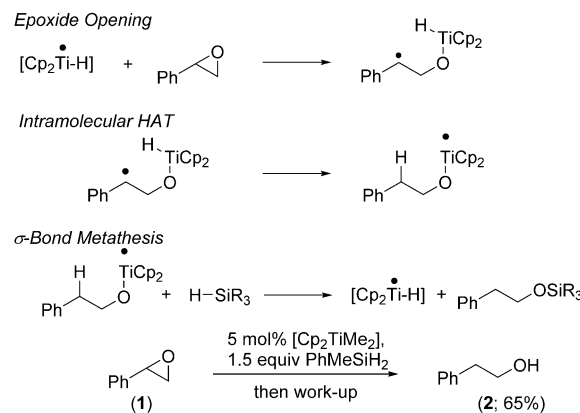
M. Bauer, Dr. R. Sure, Prof. Dr. S. Grimme
Mulliken Center for Theoretical Chemistry
Institut für Physikalische Chemie und Theoretische Chemie
Universität Bonn
Beringstraße 4, 53115 Bonn (Deutschland)

A. Meyer, Prof. Dr. O. Schiemann
Institut für Physikalische Chemie und Theoretische Chemie
Universität Bonn
Wegelerstraße 12, 53115 Bonn (Deutschland)

Prof. Dr. R. A. Flowers II
Department of Chemistry, Lehigh University
Bethlehem, PA 18015 (USA)

[†] These authors contributed equally.

Supporting information for this article can be found under:
<http://dx.doi.org/10.1002/anie.201601242>.



Scheme 1. Titanocene-catalyzed epoxide hydrosilylation.^[1a]

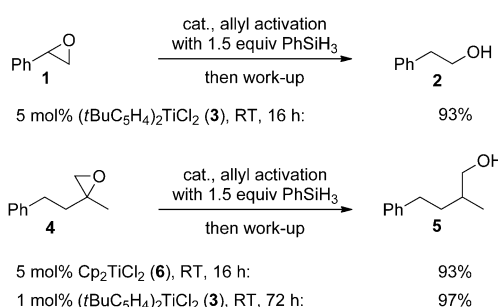
ΔG_{298} values for the σ-bond metathesis indicate that [Cp₂TiH] formation is favorable for R = Me, thermoneutral for R = Allyl, and endergonic for R = Ph with PhSiH₃. (EtO)₃SiH was predicted to be inferior. In practice, [Cp₂TiAllyl] is especially attractive since it can be prepared *in situ* by stirring Cp₂TiCl₂ (1 equiv) and AllylMgBr (2.2 equiv) in THF (1–10 min, purple reaction mixture).^[5] After the addition of PhSiH₃ (1.5 equiv with respect to the epoxide), the generation of [Cp₂TiH] (the “allyl activation”) is complete in 1–10 min (green reaction mixture).

Examples of the hydrosilylation are shown in Scheme 2. The reaction of **1** with **3** leads to an excellent result. With 1 mol % **3**, 97 % **5** was obtained (86 % **5** with 0.5 mol % (Cp₂TiOEt)₂, that is 1 mol % of Ti, and 78 % **5** with 1 mol % Cp₂TiMe₂).^[1a]

We then turned our attention to mechanistic issues and investigated whether EPR-active species^[7] are present in the solution after “allyl activation”. To this end, the activation

Cp ₂ Ti–R*THF	+ PhSiH ₃ or [(EtO) ₃ SiH]	→	Cp ₂ Ti–H*THF	+ PhSiH ₂ R or [(EtO) ₃ SiR]
	R = Me		R = Ph	R = allyl
PW6B95-D3	-4.2 (+4.3)		+2.5 (+15.0)	+0.6 (+9.7)
B3LYP-D3	-3.8 (+5.2)		+3.2 (+16.4)	+0.6 (+10.1)

Figure 1. Computed ΔG at 298.15 K for [Cp₂TiH] generation by σ-bond metathesis in THF in kcal mol⁻¹. Values in parentheses refer to (EtO)₃SiH. For comparison, data for two dispersion-corrected density functionals are given.



was conducted under the standard reaction conditions with either PhSiH₃ or PhSiD₃. The resulting X-band EPR spectra and their simulations are shown in Figure 2. Two dominating signals were observed when using PhSiH₃. The first signal is centered at $g_{\text{iso},\text{quintet}} = 1.9970$ and shows a quintet hyperfine coupling (hfc) structure with an hfc constant of 8.75 MHz. We suggest that the observed quintet is the result of adduct formation between PhSiH₃ and Cp₂TiH (Figure 2 and Sup-

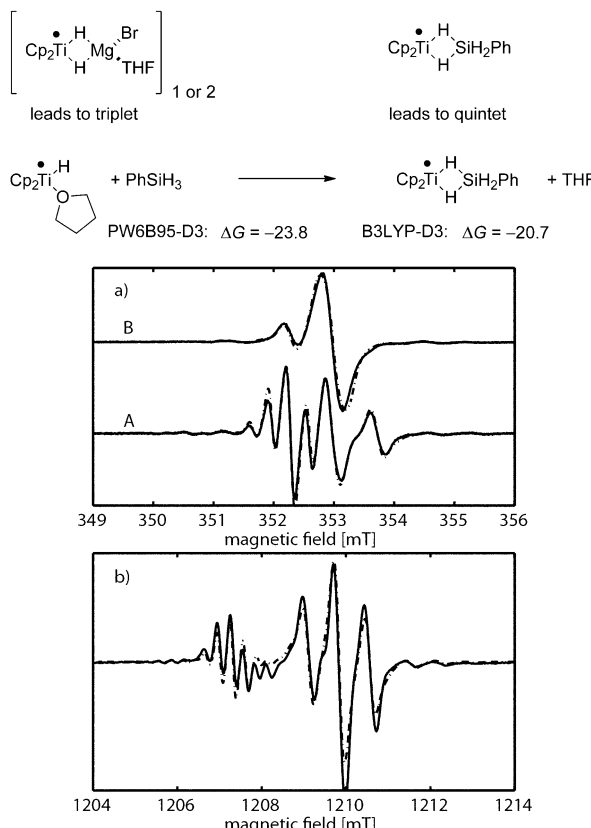


Figure 2. Proposed structures present in solution and corresponding experimental (solid lines) and simulated (dashed lines) EPR spectra after “allyl activation” at X-band (a) and Q-band (b). At X-band, PhSiH₃ (A) and PhSiD₃ (B) were used during the activation. Free energies are given in kcal mol⁻¹.

porting Information for details). Calculations show that this process is strongly exergonic. The calculated hfc constants are in qualitative agreement with the experimental values (see the Supporting Information). The other signal shows a triplet hfc structure with an hfc constant of 20.50 MHz and is centered at $g_{\text{iso},\text{triplet}} = 1.9930$. The hfc structure of both signals is absent when PhSiD₃ is used. For the species resulting in the observed triplet, we propose a complex of solvated HMgBr with Cp₂TiH or its dimer (see Figure 2 and the Supporting Information for details). The groups of Brintzinger and Mach have postulated, isolated, and characterized closely related complexes.^[5b,8] Therefore, all species detected contain Ti–H bonds.

To understand the mechanism of this reaction, a series of rate experiments were performed on the hydrosilylation of **4** through “allyl activation” of **6** with PhSiH₃. The reaction was monitored in real time through in situ IR Spectroscopy or Vis spectroscopy. Each experiment was repeated at least once. Initial experiments were designed to examine the stability of the catalyst under synthetically relevant conditions.^[9,10] The conversion of **4** into **5** in the presence of 10 mol % catalyst was monitored by following **5** and subsequently plotting **4** as a function of time (Figure 3). A higher catalyst loading was

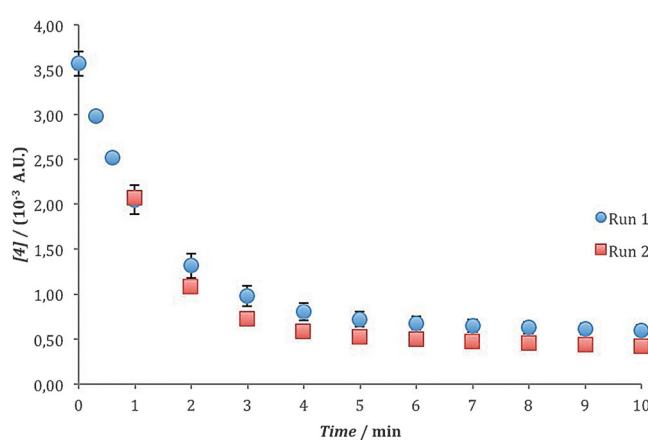


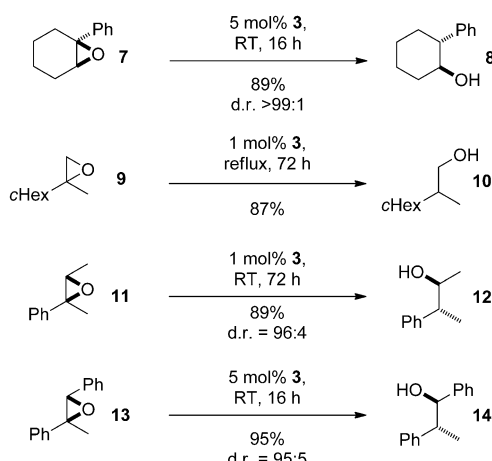
Figure 3. “Same excess” experiment. Profile of Run 1 plotted as **[4]** vs. time and the time-adjusted profile of Run 2 as **[4]** vs. adjusted time (see the Supporting Information for details).

employed to ensure reproducible detection of the titanocene species and to obtain fast turnover. When the reaction reaches the first half-life with respect to **[4]**, an equivalent amount of PhSiH₃ should be consumed and **[Ti]** should remain constant under ideal conditions. A second run was initiated under identical conditions to the first half-life of the first reaction. When the concentration data for the second run are plotted versus time and time-adjusted accordingly, the overlay is good, showing only a very slight inhibition or deactivation at the early stages of the reaction.^[11]

The rate orders with respect to the catalyst, **4**, and PhSiH₃ were determined by using the “initial rate” method. The reaction was approximately first order with respect to the catalyst, but surprisingly showed inverse order with respect to **4**.

The rate order with respect to the silane was established by varying $[PhSiH_3]$ and monitoring $[Cp_2TiH]$ through in situ Vis spectroscopy at 601 nm because of interfering silane bands in the IR spectrum. The overlap of the graphs was consistent with a rate order of zero with respect to the silane. To confirm these findings, two further sets of experiments were carried out. First, the rate order with respect to silane was additionally determined using “different excess” experiments (Supporting Information). The experiment examining the impact of $[PhSiH_3]$ confirmed that the rate order with respect to the silane is indeed zero. Second, an experiment on the hydrosilylation of **7** (Scheme 3) also established an inverse rate order with respect to the epoxide (Table 1).

Clearly, the mechanism of epoxide hydrosilylation is rather intricate. Neither epoxide opening, nor the intramolecular hydrogen atom transfer (HAT), nor σ -bond metathesis can be the rate-determining step. The formation of a resting state of the catalyst that reversibly binds the epoxide substrate without inducing ring opening must thus be responsible for the observed reaction orders. A plausible scenario is epoxide binding by Cp_2TiOR (OR is formed through epoxide opening followed by HAT, Scheme 1).



Scheme 3. Titanocene-catalyzed epoxide hydrosilylation with **3** after “allyl activation” in the presence of 1.5 equiv (second example 2.3 equiv) $PhSiH_3$.

Table 1: Rate orders with respect to the different reactants for the titanocene-catalyzed hydrosilylation of **4** after “allyl activation”. Values in parentheses refer to **7**.

Reaction component	Rate order
$[Ti]$	$1.2 \pm 0.3^{[a]}$
$PhSiH_3$	$0.1 \pm 0.4^{[b]}$
Epoxide 4 (and 7)	$-1.4 \pm 0.3^{[c]} (-1.3 \pm 0.2)^{[d]}$

[a] Conditions: Initial rate method. $[Ti]$ 3.3–13 mM, 67 mM epoxide **4**, 103 mM $PhSiH_3$. [b] Owing to interfering silane bands in the IR spectrum, this rate order was determined by in situ monitoring of the $[Ti]$ species through Vis spectroscopy. Conditions: Initial rate method. $[Ti]$ 2 mM, 37.5 mM epoxide **4**, 38.0–47.6 mM $PhSiH_3$. [c] Conditions: Initial rate method. $[Ti]$ 6.7 mM, 67–267 mM epoxide **4**, 103 mM $PhSiH_3$. [d] Conditions: Initial rate method. $[Ti]$ 6.7 mM, 67–183 mM epoxide **7**, 103 mM $PhSiH_3$.

Our calculations (Figure 4) show that $[Cp_2Ti-OEt]$ forms a more stable epoxide complex than $[Cp_2Ti-H]$. The opening of the $[Cp_2Ti-OEt]$ epoxide complex to the β -metaloxy radical is distinctly slower. In agreement with this prediction, we found that $[Cp_2TiOEt]_2$ does not open **4** (see the Supporting Information). Therefore, it seems that an epoxide complex of titanocene(III) alkoxides is indeed the resting state of this catalyst.

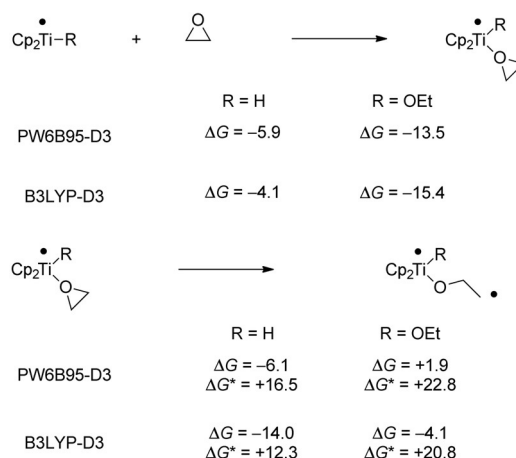


Figure 4. Computational analysis of epoxide complexation and opening by $[Cp_2Ti-H]$ and $[Cp_2Ti-OEt]$. Free energies are given in kcal mol^{-1} .

To validate this conclusion, a solution of $Cp_2TiAllyl$ was mixed with $PhSiH_3$ and **4** and immediately shock-frozen with liquid N_2 (Figure 5, black lines). Sample preparation was repeated using $PhSiH_3$ and 2,2-D₂–**4** (red lines), $PhSiD_3$ and **4** (green lines), and $PhSiD_3$ and 2,2-D₂–**4** (blue lines). The frozen solutions were subjected to pulsed Q-band EPR and electron nuclear double resonance (ENDOR) spectroscopy (Figure 5 a).^[12] The EPR spectra of the different samples are all similar and cover a field range of approximately 30 mT, with intense maxima at *g*-values of 1.9857 and 1.9651 (see the Supporting Information). The values are in the typical range for titanocenes.^[4,13] The spectra are the result of the presence of several paramagnetic species.

ENDOR spectroscopy of these samples yielded the ¹H hyperfine coupling patterns shown in Figure 5a. When 2,2-D₂–**4** was used instead of **4**, the proton resonance at an approximate hfc constant of 2.5 MHz was no longer observed. Similarly, resonances at an approximate hfc constant of 1.0 MHz were not detected with $PhSiD_3$, although the magnitude of the observed effect appeared to be weaker. The smaller hfc constant indicates a larger electron–nucleus separation. Finally, both resonances are suppressed when both reagents are deuterated. Additionally, deuteron resonances at corresponding hfc constants were observed when deuterated reagents were used (Figure 5b). The observed effects in the ENDOR spectra indicate that one of the ligands at the Ti^{III} center is the alkoxide formed after epoxide opening and HAT. Whether or not an additional epoxide is also bound to the Ti^{III} center cannot conclusively be answered by using ENDOR spectroscopy. However, the obtained spectra do not

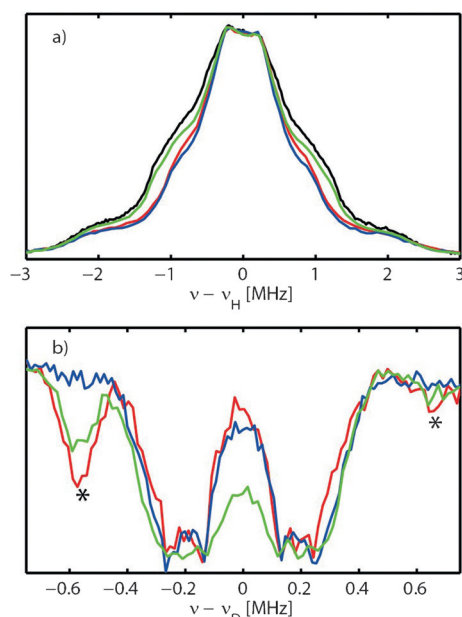


Figure 5. Q-band Davies ENDOR spectra of the protons^[12b] (a) and Mims ENDOR spectra of the deuterons^[12c] (b) of the reaction mixture using different degrees of deuteration. Black: no deuteration, red: 2,2-D₂-4, green: PhSiD₃, blue: 2,2-D₂-4, PhSiD₃. The asterisks in (b) indicate higher harmonics of the proton resonances.

contradict this interpretation. All of the computational and experimental data thus hint at the epoxide complex of the corresponding [Cp₂TiOR] as the resting state of this catalyst.

Finally, we investigated the efficiency of our reaction for the substrates shown in Scheme 3. In all cases, we obtained high yields and diastereoselectivity (when applicable).

In summary, we have designed and developed an in situ method for the generation of [Cp₂Ti-H] from Cp₂TiCl₂ or substituted titanocenes, AllylMgBr, and PhSiH₃. The system provides highly active and diastereoselective epoxide hydrosilylation and constitutes an atom-economical radical reaction.^[14] By combining kinetic, EPR, and synthetic experiments

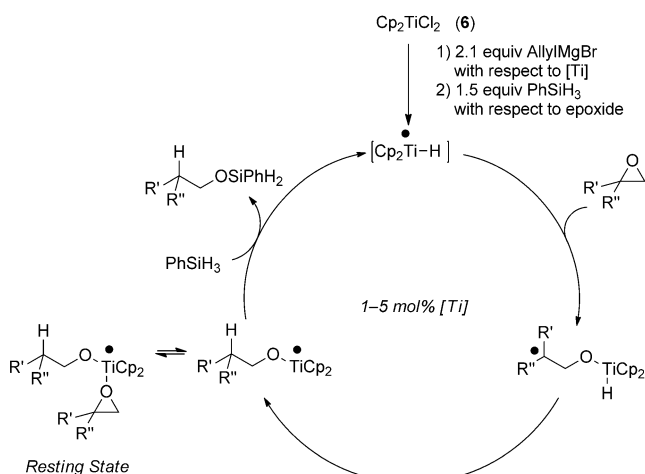


Figure 6. The catalytic cycle for epoxide hydrosilylation after “allyl activation” of 6.

ments with theoretical methods, we have shown that the catalytic cycle is rather unusual in having a resting state that leads to an inverse reaction order with respect to the epoxide (Figure 6).

Acknowledgements

We thank the DFG (SFB 813 “Chemistry at Spin Centers” and Ga 619/11-1), the Jürgen Manchot Stiftung (fellowships to S.K. and D.S.G.H.), and the National Science Foundation (CHE-1123815, R.A.F.) for financial support.

Keywords: homogeneous catalysis · hydrogen-atom transfer · hydrosilylation · radicals · titanium

How to cite: *Angew. Chem. Int. Ed.* **2016**, *55*, 7671–7675
Angew. Chem. **2016**, *128*, 7801–7805

- [1] a) A. Gansäuer, M. Klatte, G. M. Brändle, J. Friedrich, *Angew. Chem. Int. Ed.* **2012**, *51*, 8891–8894; *Angew. Chem.* **2012**, *124*, 9021–9024; b) Y.-Q. Zhang, N. Funken, P. Winterscheid, A. Gansäuer, *Angew. Chem. Int. Ed.* **2015**, *54*, 6931–6934; *Angew. Chem.* **2015**, *127*, 7035–7038.
- [2] Recent examples of titanocene(III)-catalysis: a) X. Zheng, J. He, H. H. Li, A. Wang, X. J. Dai, A. E. Wang, P. Q. Huang, *Angew. Chem. Int. Ed.* **2015**, *54*, 13739–13742; *Angew. Chem.* **2015**, *127*, 13943–13946; b) J. Streuff, M. Feurer, G. Frey, A. Steffani, S. Kaepczak, J. Weweler, L. H. Leijendekker, D. Krakert, D. A. Plattner, H. Dietmar, *J. Am. Chem. Soc.* **2015**, *137*, 14396–14405; c) J. Streuff, A. Gansäuer, *Angew. Chem. Int. Ed.* **2015**, *54*, 14232–14242; *Angew. Chem.* **2015**, *127*, 14438–14448.
- [3] a) C. Aitken, J. F. Harrod, *J. Organomet. Chem.* **1985**, *279*, C11–C13; b) C. A. Willoughby, S. L. Buchwald, *J. Am. Chem. Soc.* **1994**, *116*, 11703–11714; c) C. A. Willoughby, S. L. Buchwald, *J. Am. Chem. Soc.* **1994**, *116*, 8952–8965; d) S. Xin, J. F. Harrod, *Can. J. Chem.* **1995**, *73*, 999–1002; e) K. Rahimian, J. F. Harrod, *Inorg. Chim. Acta* **1998**, *270*, 330–336; f) J. Yun, S. L. Buchwald, *J. Am. Chem. Soc.* **1999**, *121*, 5640–5644.
- [4] E. Samuel, J. F. Harrod, D. Gourier, Y. Dromzee, F. Robert, Y. Jeannin, *Inorg. Chem.* **1992**, *31*, 3252–3259.
- [5] a) H. A. Martin, F. Jellinek, *J. Organomet. Chem.* **1967**, *8*, 115–128; b) H. H. Brintzinger, *J. Am. Chem. Soc.* **1967**, *89*, 6871–6877; c) E. Klei, J. H. Teuben, *J. Organomet. Chem.* **1980**, *188*, 97–107; d) E. Klei, J. H. Teuben, H. J. de Liefde Meijer, E. J. Kwak, *J. Organomet. Chem.* **1982**, *224*, 327–339.
- [6] The TURBOMOLE 7.0 program package^[a] was employed for gas-phase geometry optimizations and calculations of thermochemical corrections at the TPSS^[b]-D3^[c,d]/def2-TZVP^[e] level, as well as single-point energies at the PW6B95^[f]-D3 or B3LYP^[g,h]-D3 level with the def2-QZVP^[e] basis set. Solvation contributions to ΔG were included through the COSMO-RS^[i,j] continuum solvation model. a) F. Furche, R. Ahlrichs, C. Hättig, W. Klopper, M. Sierka, F. Weigend, *WIREs Comput. Mol. Sci.* **2014**, *4*, 91–100; b) J. Tao, J. Perdew, V. Staroverov, G. Scuseria, *Phys. Rev. Lett.* **2003**, *91*, 146401; c) S. Grimme, J. Antony, S. Ehrlich, H. Krieg, *J. Chem. Phys.* **2010**, *132*, 154104; d) S. Grimme, S. Ehrlich, L. Goerigk, *J. Comput. Chem.* **2011**, *32*, 1456–1465; e) F. Weigend, R. Ahlrichs, *Phys. Chem. Chem. Phys.* **2005**, *7*, 3297–3305; f) Y. Zhao, D. G. Truhlar, *J. Phys. Chem. A* **2005**, *109*, 5656–5667; g) A. D. Becke, *J. Chem. Phys.* **1993**, *98*, 5648–5652; h) P. J. Stephens, J. Devlin, C. F. Chabalowski, M. J. Frisch, *J. Phys. Chem.* **1994**, *98*, 11623–11627; i) A. Klamt, *J. Chem. Phys.* **1995**, *99*, 2224–2235; j) F. Eckert, A. Klamt, *AIChE J.* **2002**, *48*, 369–385.

- [7] *Multifrequency Electron Paramagnetic Resonance, Theory and Applications* (Ed.: S. K. Misra), Wiley-VCH, Weinheim, **2011**.
- [8] a) H. Brintzinger, *J. Am. Chem. Soc.* **1966**, *88*, 4306–4307; b) V. Kupfer, U. Thewalt, M. Horácek, L. Petrusová, K. Mach, *Inorg. Chem. Commun.* **1999**, *2*, 540–544; c) S. I. Troyanov, V. Varga, K. Mach, *J. Organomet. Chem.* **1993**, *461*, 85–90; d) R. Gyepes, K. Mach, I. Císařová, J. Loub, J. Hiller, P. Sindelár, *J. Organomet. Chem.* **1995**, *497*, 33–41.
- [9] Selected reviews on RPKA: a) D. G. Blackmond, *Angew. Chem. Int. Ed.* **2005**, *44*, 4302–4320; *Angew. Chem.* **2005**, *117*, 4374–4393; b) D. G. Blackmond, *J. Am. Chem. Soc.* **2015**, *137*, 10852–10866.
- [10] Recent examples of RPKA in practice: a) A. J. Wagner, S. D. Rychnovsky, *Org. Lett.* **2013**, *15*, 5504–5507; b) M. Scott, A. Sud, E. Boess, M. Klussmann, *J. Org. Chem.* **2014**, *79*, 12033–12040; c) N. R. Patel, R. A. Flowers II, *J. Org. Chem.* **2015**, *80*, 5834–5841; d) Y. N. Ji, R. E. Plata, C. S. Regens, M. Hay, M. Schmidt, T. Razler, Y. P. Qiu, P. Geng, Y. Hsiao, T. Rosner, M. D. Eastgate, D. G. Blackmond, *J. Am. Chem. Soc.* **2015**, *137*, 13272–13281; e) P. Ruiz-Castillo, D. G. Blackmond, S. L. Buchwald, *J. Am. Chem. Soc.* **2015**, *137*, 3085–3092.
- [11] a) R. D. Baxter, D. Sale, K. M. Engle, J.-Q. Yu, D. G. Blackmond, *J. Am. Chem. Soc.* **2012**, *134*, 4600–4606; b) J. J. Devry III, J. J. Douglas, J. D. Nguyen, K. P. Cole, R. A. Flowers II, C. R. J. Stephenson, *Chem. Sci.* **2015**, *6*, 537–541.
- [12] a) A. Schweiger, G. Jeschke, *Principles of electron paramagnetic resonance*, Oxford University Press, Oxford, **2005**; b) E. R. Davies, *Phys. Lett. A* **1974**, *47*, 1–2; c) W. B. Mims, *Proc. R. Soc. London Ser. A* **1965**, *283*, 452–457.
- [13] a) W. W. Lukens, Jr., M. R. Smith III, R. A. Andersen, *J. Am. Chem. Soc.* **1996**, *118*, 1719–1728; b) A. Cangönül, M. Behlendorf, A. Gansäuer, M. van Gastel, *Inorg. Chem.* **2013**, *52*, 11859–11866.
- [14] a) A. Gansäuer, A. Fleckhaus, M. A. Lafont, A. Okkel, K. Kotsis, A. Anoop, F. Neese, *J. Am. Chem. Soc.* **2009**, *131*, 16989–16999; b) A. Gansäuer, M. Behlendorf, D. von Laufenberg, A. Fleckhaus, C. Kube, D. V. Sadasivam, R. A. Flowers II, *Angew. Chem. Int. Ed.* **2012**, *51*, 4739–4742; *Angew. Chem.* **2012**, *124*, 4819–4823; c) A. Gansäuer, C. Kube, K. Daasbjerg, R. Sure, S. Grimme, G. D. Fianu, D. V. Sadasivam, R. A. Flowers II, *J. Am. Chem. Soc.* **2014**, *136*, 1663–1671; d) A. Gansäuer, D. von Laufenberg, C. Kube, T. Dahmen, A. Michelmann, M. Behlendorf, R. Sure, M. Seddiqzai, S. Grimme, D. V. Sadasivam, G. D. Fianu, R. A. Flowers II, *Chem. Eur. J.* **2015**, *21*, 280–289; e) A. Gansäuer, S. Hildebrandt, A. Michelmann, T. Dahmen, D. von Laufenberg, C. Kube, G. D. Fianu, R. A. Flowers II, *Angew. Chem. Int. Ed.* **2015**, *54*, 7003–7006; *Angew. Chem.* **2015**, *127*, 7109–7112.

Received: February 3, 2016

Published online: April 29, 2016